Molecular Crystals and Liquid Crystals

Publication details, including instructions for authors and subscription information:
http://www.tandfonline.com/loi/gmcl20

Current Assymetry Caused by Molecule-Electrode Contacts

E. G. Petrov [a] , Ya. R. Zelinskyy [a] & V. I. Teslenko [a]

[a] Bogolyubov Institute for Theoretical Physics, National Academy of Sciences of Ukraine, Kyiv, Ukraine

Version of record first published: 22 Sep 2010

To cite this article: E. G. Petrov, Ya. R. Zelinskyy & V. I. Teslenko (2007): Current Assymetry Caused by Molecule-Electrode Contacts, Molecular Crystals and Liquid Crystals, 467:1, 93-106

To link to this article: http://dx.doi.org/10.1080/15421400701220999

Mol. Cryst. Liq. Cryst., Vol. 467, pp. 93–106, 2007

ISSN: 1542-1406 print/1563-5287 online
DOI: 10.1080/15421400701220999

Current Assymetry Caused by Molecule–Electrode Contacts

E. G. Petrov
Ya. R. Zelinskyy
V. I. Teslenko
Bogolyubov Institute for Theoretical Physics, National Academy of Sciences of Ukraine, Kyiv, Ukraine

The current–voltage ($I-V$) characteristics and the conductance of a molecular wire are evaluated under the condition of a weak electron-vibrational coupling. It is shown that, in the case of strong couplings between the molecular wire and the electrodes, the current formation is associated with a complicated mixture of superexchange (elastic) and sequential (inelastic) transfer processes just within the molecular wire. At a large energy gap between the level positions of the terminal and interior wire units, the transfer along a sequential electronic pathway becomes noneffective. Therefore, the current is mainly determined by an elastic mechanism. If molecule–electrode couplings are weak, the $I-V$ characteristics are connected with the interfacial charge hopping processes limiting the common charge transmission.

Keywords: interelectrode current; kinetic equations; molecular wire; voltage bias

PACS: 05.20.Dd 05.60. +w

I. INTRODUCTION

There is a currently intense interest in the studies of the electrical properties of single molecules by both fundamental and practical reasons. It is due to their potential application as counterparts of molecular electronic devices [1–4]. The improvement of experimental technique based on using the scanning tunneling microscopy [5,6],

The work is supported in part by the Found of Fundamental Research of the NASU.
Address correspondence to E. G. Petrov, Bogolyubou Institute for Theoretical Physics, National Academy of Sciences of Ukraine, Metrolohichna Str., Kyiv 03143, Ukraine. E-mail: epetov@bitp.kiev.ua

conducting atomic force microscopy [7], and mechanically controllable break junction technique [8] opens a direct way to the investigation of the conductance properties of single molecules. Experimental studies clearly show that, in most cases, the current–voltage ($I-V$) characteristics of single molecules exhibit a nonlinear behavior including such effects as a molecular rectification [9,10], a negative differential resistance [11], a switching [12,13], and memory effects [14]. Such a behavior is caused by not only a complicated electronic structure of the investigated molecules but the molecule–electrode interaction as well. It has been pointed out that the conductance is especially sensitive to microscopic details of the molecule–electrode contacts. Therefore, the character of interfacial reactions between the metal surface and the molecule attached plays a key role in the charge transport across the molecular junctions [15,16]. In common, one can distinguish three determining factors (related to the molecule–electrode interface) which control the conductance properties of single molecules and molecular wires: a geometry variation, a chemical nature of terminal groups/atoms, and a strength of molecule–electrode interaction. In particular, the presence of metallic electrodes can strongly modify molecular electronic levels which, additionally, become broadened.

In the present communication, the role of electrode–molecule contacts in the formation of the current through a short molecular wire is studied theoretically with the use of the density matrix method. The previous theoretical studies based on the nonequilibrium Green's function formalism have been applied to the investigation of the molecule–electrode interface of α,α'- *xylyl*-dithiol molecular wires [17]. It has been shown that varying the surface geometry does not affect the conductance in a significant way. Additionally, a strong dependence of the conductance on the chemical nature of the terminal atoms, as well as on the electrode–terminal site distance, has been established. A minor role of the geometric position of the terminal atoms with respect to the metallic surface has been demonstrated numerically with the use of the density functional theory. [The theory has been applied to the investigation of self-assembled monolayers of the thiolated conjugated wires attached on a gold surface [18].] It has been shown that a small change in the orientation of the molecular wire with respect to the surface does not modify drastically the electronic structure of the molecular wire. In contrast to the minor role of the geometric position of a metal/molecular complex on conductance properties of the complex, a strong influence of the electronic interaction between a molecular wire and a metal surface has been found. This interaction modifies locally the electronic structure of a metal surface and leads, thus, to a strong modification and a broadening of

the electronic levels of the molecule [19]. Additionally, the extent of the molecule–electrode coupling at metal–molecule interfaces can lead to the current rectification even in a symmetric system [9,20]. In particular, the experimental and theoretical studies of the charge transport across the metal–molecule–metal junctions formed from two oligo(phenylene ethylene) molecules manifest a control of the current rectification by a change of the coupling at the metal-molecule contact [9]. Another theoretical results show that a similar rectification can result from unequal voltage drops and injection barriers at the two metal-molecule contacts [21–23]. The results of theoretical studies based on the nonequilibrium density matrix method show that the rectification effect can be associated with the asymmetric charging of the molecule by transferred electrons [24,25]. Such a kinetic rectification can be especially significant on the resonant transmission through the isolated molecular levels [26,27].

The goal of the present article is to clarify the influence of the molecule–electrode interface on rectification properties of a short molecular wire with strongly energetically positioned levels belonging the interior wire units. Two limiting cases of strong and weak molecule–electrode couplings are considered. In both cases, the analytic expressions for the current are derived and the current–voltage characteristics of the wire along with the wire conductance are analyzed.

II. MODEL AND THEORY

To study the effect of metallic electrodes on the current-voltage characteristics of the molecule, we apply a model of molecular wire consisting of the terminal donor (D) and acceptor (A) sites, as well as two interior sites of electron localization ($n = 1$ and $n = 2$), Figure 1. In the model, the

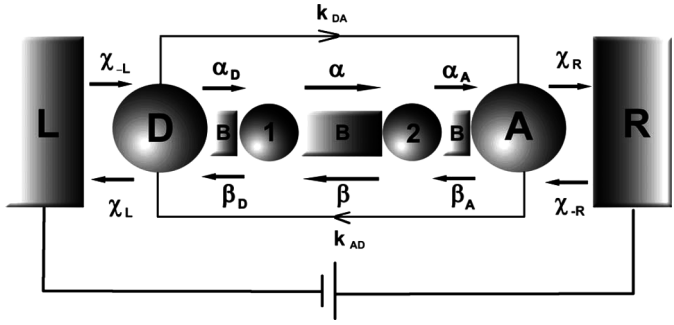

FIGURE 1 Kinetic scheme of electron transmission through a short molecular wire embedded between two metallic electrodes.

electron transfer (ET) between the electrodes (denoted by the symbols **L** and **R**) and the corresponding terminal sites D and A is characterized by single-electron hopping transfer rates $\chi_{L(R)}$ and $\chi_{-L(-R)}$. The transfer rates $\alpha_D,\ \alpha,\ \alpha_A$ and $\beta_D,\ \beta,\ \beta_A$ characterize the electron hopping between the neighboring sites of electron localization within the wire. It is assumed in the model that the terminal sites differ chemically on the interior sites so that the lowest unoccupied molecular orbital (LUMO) levels of the terminal units are positioned strongly below the LUMO levels of the interior units [28]. Such a position of the levels supposes the appearance of a specific superexchange interaction between the D and A sites. The respective superexchange forward (k_{DA}) and backward (k_{AD}) transfer rates characterize a distant one-step electron hopping between the terminal units. Thus, the current is formed by the motion of single electrons along the sequential and the superexchange pathways.

We derive the current on the base of the general expression

$$I = -e\dot{N}_L(t), \tag{1}$$

where e denotes the absolute value of the electron charge, and $\dot{N}_L(t)$ $(= -\dot{N}_R(t))$ is the time-derivative of the number of electrons present at the left (right) electrode. To derive $\dot{N}_L(t)$, we note the fact of a small population of the interior wire sites. It is due to a higher position of the LUMO levels belonging the interior sites relative to the LUMO levels of the terminal sites. In addition, we consider only a nonadiabatic regime of the charge transfer when the ET occurs on the background of the fast vibration relaxaion within each electronic term. This allows us to use a system of linear kinetic equations derived in Ref. [29] for integral electronic populations of the wire sites, $P_n(t)$, $(n = D, 1, 2, A)$. In our notations, the system reads

$$\begin{aligned}
\dot{N}_L(t) &= -\chi_L + (\Gamma_L/\hbar)P_D(t),\\
\dot{P}_D(t) &= -((\Gamma_L/\hbar) + \alpha_D + k_{DA})P_D(t) + \chi_L + \beta_D P_1(t) + k_{AD}P_A(t),\\
\dot{P}_1(t) &= -(\alpha + \beta_D)P_1(t) + \alpha_D P_D(t) + \beta P_2(t),\\
\dot{P}_2(t) &= -(\alpha_A + \beta)P_2(t) + \alpha P_1(t) + \beta_A P_A(t),\\
\dot{P}_A(t) &= -((\Gamma_R/\hbar) + \beta_A + k_{AD})P_A(t) + \chi_R + \alpha_A P_A(t) + k_{DA}P_D(t),\\
\dot{N}_R(t) &= -\chi_R + (\Gamma_R/\hbar)P_A(t).
\end{aligned} \tag{2}$$

In Eq. (2), the width parameters

$$\Gamma_L \equiv \hbar(\chi_L + \chi_{-L}), \quad \Gamma_R \equiv \hbar(\chi_R + \chi_{-R}) \tag{3}$$

determine the broadening of the D and A terminal electronic wire levels. The broadenings are caused by the interaction of the noted

levels with the conduction band levels of the left and right electrodes, as well as by the coupling to vibrational modes.

We restrict ourselves by consideration of the stationary case where $\dot{P}_n(t) = 0$. This yields $\dot{N}_L = -\dot{N}_R = \text{const}$. At the stationary regime of charge transmission, system (2) is reduced to the system of linear algebraic equations

$$\sum_{m=D,1,2,A} A_{nm} P_m = C_n, \quad (n = D, 1, 2, A). \tag{4}$$

Here, A_{nm} is the basic matrix of the linear system (2), and $C_n = \chi_L \delta_{nD} + \chi_R \delta_{nA}$. Solving system (2) and substituting the reading form of the P_D in the first equation of system (2), we obtain the analytic expression for the stationary inter-electrode current,

$$I = \theta(V) I_+(V) + (1 - \theta(V)) I_-(V), \tag{5}$$

where $I_+(V)$ and $I_-(V)$ are the current components at positive and negative voltages, $\theta(v)$ is the Heaviside's unit function. At $V > 0$, the current appears as

$$I_+(V) = I_0 2\pi (1 - e^{-eV/k_B T}) \frac{\hbar \chi_L}{\Gamma_L} \frac{\hbar K_+}{A}, \tag{6}$$

[Note the introduction of the current unit $I_0 \equiv e/\pi\hbar \times 1\,\text{eV} \approx 80\ \mu\text{A}$. It supposes that the quantities $\Gamma_{L(R)}, \hbar\chi_{L(R)}, \hbar k_{DA}, \hbar k_{AD}, \hbar\alpha$, etc. have to be given in electron-volts]. In Eq. (6),

$$K_+ = k_{DA}\left(1 + \frac{\alpha}{\beta_D} + \frac{\beta}{\alpha_A}\right) + \frac{\alpha\alpha_D}{\beta_D} \tag{7}$$

and

$$A = \left(1 + \frac{\hbar k_{DA}}{\Gamma_L} + \frac{\hbar k_{AD}}{\Gamma_R}\right)\left(1 + \frac{\alpha}{\beta_D} + \frac{\beta}{\alpha_A}\right) + \frac{\hbar\alpha\alpha_D}{\Gamma_L\beta_D} + \frac{\hbar\beta\beta_A}{\Gamma_R\alpha_A}. \tag{8}$$

Analogously, at negative voltages ($V < 0$), we get

$$I_-(V) = -I_0 2\pi (1 - e^{-e|V|/k_B T}) \frac{\hbar \chi_R}{\Gamma_R} \frac{\hbar K_-}{A}, \tag{9}$$

$$K_- = k_{AD}\left(1 + \frac{\alpha}{\beta_D} + \frac{\beta}{\alpha_A}\right) + \frac{\beta\beta_A}{\alpha_A}. \tag{10}$$

III. RATE CONSTANTS

To analyze the current–voltage characteristics, one has to specify both the expression for rate constants and the location of electronic density over the wire. In the case of nonadiabatic ET under consideration, the

intersite electronic matrix elements $V_{D1}, V_B \equiv V_{12}$, and V_{2A} are assumed to be small, so that all molecular electronic terms can be referred to the sites of electron localization. Therefore, just the site energies E_m determine the direction of the ET process under the voltage bias. To derive a voltage shift of the E_m, we suppose that the "center of gravity" of the electronic density of each site is positioned just at the center of the site. Let l_L and l_R be the distances between the terminal sites and the respective adjacent electrodes, and let l_W be the distance between the wire units. Denoting the electrode–electrode distance as $l \equiv l_L + 3l_W + l_A$, we determine the voltage division factors as $\eta_L \equiv l_L/l,\ \eta_R \equiv l_R/l,$ and $\eta_W \equiv l_W/l$. With the introduction of these factors, the shift of energy levels is determined by the expressions

$$\begin{aligned} E_D &= E_D^0 - eV\eta_L, \\ E_n &= E_n^0 - eV(\eta_L + n\eta_W), \quad (n = 1, 2), \\ E_A &= E_A^0 - eV(1 - \eta_R). \end{aligned} \tag{11}$$

To specify the ET rate constants, we employ the well-known Marcus form [30] which can be represented for the forward ET rates as

$$\beta_D = \frac{2\pi}{\hbar}\frac{|V_{1D}|^2}{\sqrt{4\pi\lambda_D k_B T}}\exp\left[-\frac{(\Delta E_D - \lambda_{1D})^2}{4\lambda_D k_B T}\right], \tag{12}$$

$$\alpha_A = \frac{2\pi}{\hbar}\frac{|V_{2A}|^2}{\sqrt{4\pi\lambda_A k_B T}}\exp\left[-\frac{(\Delta E_A - \lambda_{2A})^2}{4\lambda_{2A} k_B T}\right], \tag{13}$$

$$\alpha = \frac{2\pi}{\hbar}\frac{|V_B|^2}{\sqrt{4\pi\lambda_W k_B T}}\exp\left[-\frac{(eV\eta_W - \lambda_B)^2}{4\lambda_W k_B T}\right], \tag{14}$$

$$k_{DA} = \frac{2\pi}{\hbar}\frac{|V_{DA}|^2}{\sqrt{4\pi\lambda_{DA} k_B T}}\exp\left[-\frac{(\Delta E_{DA} - \lambda_{DA})^2}{4\lambda_{DA} k_B T}\right]. \tag{15}$$

The backward rate constants are expressed via the forward ones with the relations

$$\alpha_D = \beta_D \exp[-\Delta E_D/k_{\mathrm{B}}T], \tag{16}$$

$$\beta_A = \alpha_A \exp[-\Delta E_A/k_{\mathrm{B}}T], \tag{17}$$

$$\beta = \alpha \exp[-eV\eta_W/k_{\mathrm{B}}T], \tag{18}$$

$$k_{AD} = k_{DA} \exp[-\Delta E_{DA}/k_{\mathrm{B}}T]. \tag{19}$$

In Eqs. (12)–(19), energy gaps are determined by the expressions

$$\begin{aligned} \Delta E_D &= E_1 - E_D = \Delta E_D^0 - eV\eta_W, \\ \Delta E_A &= E_2 - E_A = \Delta E_A^0 + eV\eta_W, \\ \Delta E_{DA} &= E_D - E_A = \Delta E_{DA}^0 + eV(1 - \eta_L - \eta_R). \end{aligned} \tag{20}$$

The quantities $\lambda_{D(A)}$ and λ_{DA} are the reorganization energies attributed to the transitions $D(A) \to 1(2)$ and $D \to A$, respectively, whereas λ_W is the reorganization energy associated with the transition between the interior wire sites. We also introduced the gaps between the unbiased LUMO levels of the 1-st interior site and the D unit ($\Delta E_D^0 \equiv E_1^0 - E_D^0$), as well as between the 2-nd interior site and the A unit ($\Delta E_A^0 \equiv E_2^0 - E_A^0$). The unbiased driving force of the D–A ET process is denoted as $E_{DA}^0 \equiv E_D^0 - E_A^0$.

In Eq. (15), the square of the transition matrix element between the terminal sites appears as [31]

$$|V_{DA}(V)|^2 = \frac{|V_{1D}V_BV_{2A}|^2}{\prod_{m=1,2}\Delta E_{mD}\Delta E_{mA}}. \tag{21}$$

This quantity depends on a voltage bias via the energy gaps $\Delta E_{mD} \equiv E_m - E_D$ and $\Delta E_{mA} \equiv E_m - E_A$, where the site energies are given by Eq. (11). With the introduction of the factors $\phi_D(V) = -3eV\eta_W/\Delta E_D^0$ and $\phi_A(V) = +3eV\eta_W/\Delta E_A^0$ [32], quantity (21) can be rewritten in a more compact form as

$$|V_{DA}(V)|^2 = |V_{DA}(0)|^2 e^{\phi_D(V)+\phi_A(V)}, \tag{22}$$

where

$$|V_{DA}(0)|^2 \equiv \frac{|V_{1D}V_{2A}|^2}{\Delta E_D^0 \Delta E_A^0}\left(\frac{V_B}{\sqrt{\Delta E_D^0 \Delta E_A^0}}\right)^2 \tag{23}$$

is the square of the superexchange matrix element in the absence of an electric field. As to the wire-electrode transfer rates, we take them in the form [25,26]

$$\begin{aligned} \chi_{L(R)} &= \frac{1}{\hbar}\Gamma_{L(R)} n_F(\Delta E_{L(R)}), \\ \chi_{-L(-R)} &= \frac{1}{\hbar}\Gamma_{L(R)}(1 - n_F(\Delta E_{L(R)})) \end{aligned} \tag{24}$$

valid at a small electron-vibrational coupling. In Eq. (24), we use the Fermi distribution function defined as

$$n_F(\Delta E_{L(R)}) = [\exp(\Delta E_{L(R)}/k_BT) + 1]^{-1} \tag{25}$$

with

$$\Delta E_L = \Delta E_L^0 - eV\eta_L, \quad \Delta E_R = \Delta E_R^0 + eV\eta_R \tag{26}$$

being the energy gaps that exist between the terminal site levels and the respective Fermi levels ($\Delta E_{L(R)}^0 = E_{D(A)}^0 - E_F$ is the unbiased energy gap).

IV. SIMPLIFIED EXPRESSIONS FOR THE CURRENT

The general analytic expressions for the current, Eqs. (5)–(10), allows us to describe the current–voltage characteristics at different relations between the hopping rate constants. But, it becomes useful to have at hand also simpler versions suitable for the analysis of peculiar cases. In what follows, we consider the limiting cases of strong and weak molecule–electrode couplings.

Strong Molecule–Electrode Coupling

In the case of the strong coupling between the electrode and the respective terminal site, the following inequalities are fulfilled:

$$k_{DA}, \alpha_D \ll \Gamma_L/\hbar, \quad k_{AD}, \beta_A \ll \Gamma_R/\hbar. \tag{27}$$

This case corresponds to fast electron hoppings between the terminal wire units and the adjacent metallic electrodes as compared to the hoppings between the wire units. At such a regime of charge transmission, the general expression for the current is reduced to the sum of two independent contributions,

$$I = I_{sup}(V) + I_{seq}(V). \tag{28}$$

The superexchange contribution reads

$$I_{sup}(V) = e\left[1 - e^{-e|V|/k_BT}\right]\left[\theta(V)\frac{\chi_L}{\Gamma_L}k_{DA} - (1 - \theta(V))\frac{\chi_R}{\Gamma_R}k_{AD}\right]. \tag{29}$$

[Superexchange D–A coupling exhibits itself through the distant rate constants k_{DA} and k_{AD}, cf. Eqs. (15) and (19).] The sequential contribution

$$I_{seq}(V) = I_0 2\pi \frac{1 - e^{-e|V|/k_BT}}{\alpha_A\beta_D + \alpha\alpha_A + \beta_D\beta} \times \left[\theta(V)\frac{\hbar^2\chi_L}{\Gamma_L}\alpha_D\alpha\alpha_A + (\theta(V) - 1)\frac{\hbar^2\chi_R}{\Gamma_R}\beta_D\beta\beta_A\right] \tag{30}$$

is specified exclusively by the hopping transfer rates (cf. Eqs. (12)–(14) and (16)–(18)).

Weak Molecular–Electrode Coupling

At a weak molecule–electrode coupling where

$$k_{DA}, \alpha_D \gg \Gamma_L/\hbar, \quad k_{AD}, \beta_A \gg \Gamma_R/\hbar, \tag{31}$$

the current components (6) and (9) are reduced to the form

$$\begin{aligned} I_+ \equiv I_+(V) &\approx I_0 2\pi(1 - e^{-eV/k_BT})\frac{\hbar\chi_L}{\Gamma_L}\frac{\hbar K_+}{\hbar K_+/\Gamma_L + \hbar K_-/\Gamma_R}, \\ I_- \equiv I_-(V) &\approx -I_0 2\pi(1 - e^{-e|V|/k_BT})\frac{\hbar\chi_R}{\Gamma_R}\frac{\hbar K_-}{\hbar K_+/\Gamma_L + \hbar K_-/\Gamma_R}. \end{aligned} \tag{32}$$

The voltage dependence of the current is concentrated in the effective rates K_+ and K_- defined by Eqs. (7) and (10), respectively. With taking into account the relations between the backward and forward transfer rates, cf. Eqs. (16)–(19), expression (32) is transformed to the form

$$\begin{aligned} I_+ &\approx I_0 2\pi(1 - e^{-eV/k_BT})\frac{\hbar\chi_L}{\Gamma_L}\frac{\hbar}{(\hbar/\Gamma_L) + (\hbar/\Gamma_R)e^{-\Delta E_{DA}/k_BT}}, \quad (V > 0), \\ I_- &\approx -I_0 2\pi(1 - e^{-e|V|/k_BT})\frac{\hbar\chi_R}{\Gamma_R}\frac{\hbar}{(\hbar/\Gamma_L)e^{-\Delta E_{AD}/k_BT} + (\hbar/\Gamma_R)}, \quad (V < 0). \end{aligned} \tag{33}$$

which is more suitable for the discussion of the results.

V. DISCUSSION

The analytic expressions, Eq. (5) and Eqs. (6)–(9) allow us to analyze both the I–V characteristics and the conductance $dI(V)/dV$ of a molecular wire at different values of the physical parameters. Figure 2 displays the strong current rectification effect caused by the asymmetry of the coupling to the electrodes. When molecule–electrode couplings are strong so that relation (27) is fulfilled, the interelectrode current appears as the sum of superexchange, Eq. (29), and sequential, Eq. (30), contributions. But, it has been already established [29,32] that, in the case of a short molecular wire, the superexchange component of the current dominates in the total current so that $I(V) \approx I_{sup}(V)$. In what follows, just such a situation is considered only.

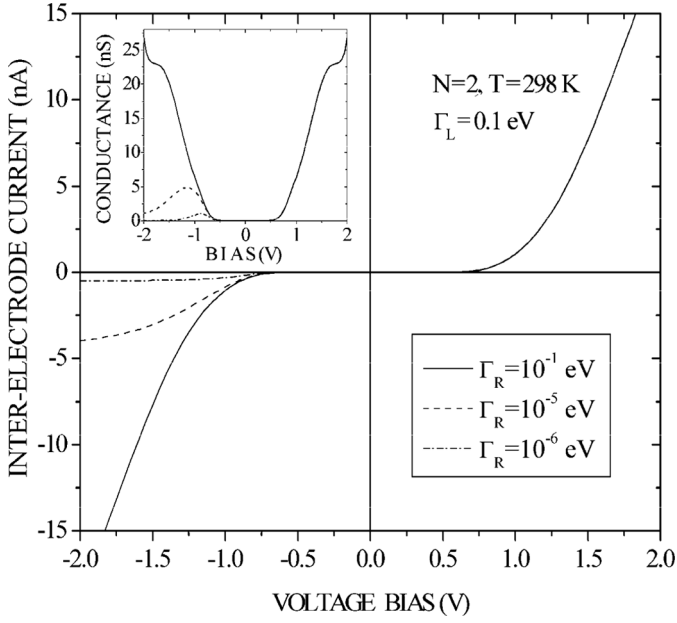

FIGURE 2 Current–voltage and conductance (cf. the insert) characteristics of a linear molecular wire with two terminal (D) and (A) and two interior units. The calculations are performed according to Eq. (5) with the following parameters: $V_{D1} = V_{2A} = 0.07\,\text{eV}, V_B = 0.05\,\text{eV}$, $\omega_{D1} = \omega_{12} = \omega_{2A} = 50\text{cm}^{-1}$, $\lambda_{D1} = \lambda_{2A} = 1.2\,\text{eV}, \lambda_B = 0.6\,\text{eV}, \lambda_{DA} = 0.9\,\text{eV}$, $\Delta E_{DF} = \Delta E_{AF} = 0.2\,\text{eV}$, $\eta_R = \eta_L = 0.25$, $\eta_B = 0.17$, $\Delta E_{D1} = \Delta E_{2A} = 0.8\,\text{eV}$, $\Gamma_L = \Gamma_R = 0.1\,\text{eV}$, $T = 298\text{K}$. The strong current rectification caused by the asymmetry in molecule–electrode couplings is shown.

Figure 2 shows the rectification ratio (RR),

$$RR = \frac{I_+(V)}{|I_-(V)|}, \tag{34}$$

against the applied voltage at strong molecule–electrode couplings. The ratio becomes rather large at a pronounced asymmetry in the molecule–electrode couplings, i.e., at a great difference between the partial broadenings (the case $\Gamma_L \gg \Gamma_R$ is manifested). The RR increases with the absolute value of the applied voltage. [In Fig. 3, the RR becomes especially large at $V > 1$ V].

In the case of weak molecule–electrode couplings, the interelectrode current can be calculated with the use of the simple expression (33). Figure 4 displays the rectification effect which is associated now with

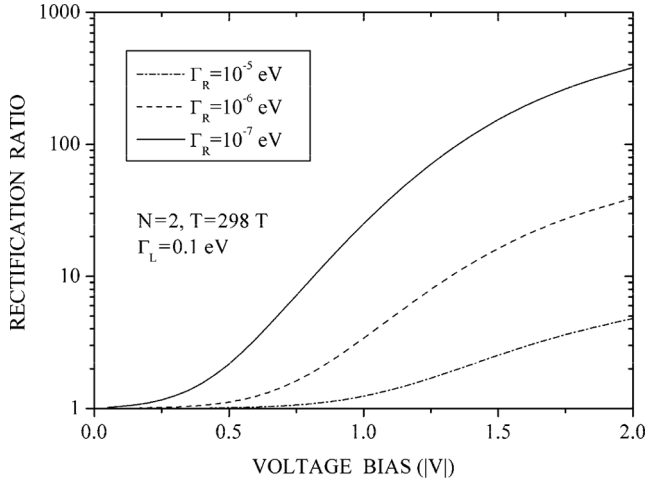

FIGURE 3 Rectification ratio against the applied voltage. The calculations are performed according to Eq. (34). The chosen parameters are the same as those in Figure 2.

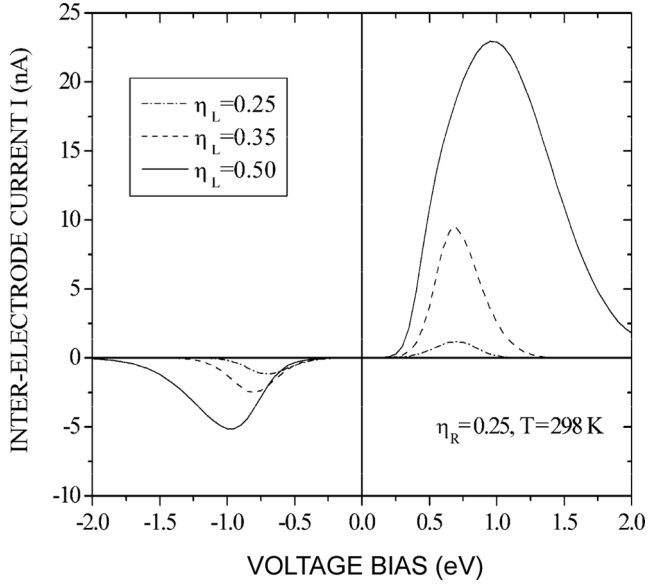

FIGURE 4 Current–voltage characteristics of a short molecular wire at weak molecule–electrode couplings. The rectification effect is caused by the difference in values of the voltage division factors. The chosen parameters are the same as those in Figure 2.

different values of the voltage division factors η_L and η_R (we recall that these factors determine the level shifts of the terminal groups with respect to the Fermi levels of the adjacent electrodes). When a voltage bias strongly exceeds a thermal energy, so that $eV \gg k_BT$, and if, additionally, $\exp(-\Delta E_{DA}/k_BT) \ll 1$ (at $V > 0$)and exp $(-\Delta E_{AD}/k_BT) \ll 1$ (at $V < 0$), we obtain the following approximation for the forward and the backward current components:

$$I_+(V) \approx I_0 2\pi\Gamma_L n_F(\Delta E_L),$$
$$I_-(V) \approx -I_0 2\pi\Gamma_R n_F(\Delta E_R). \tag{35}$$

Now, the interelectrode current depends strongly on the Fermi distribution functions $n_F(\Delta E_L)$ and $n_F(\Delta E_R)$, as well as the partial level broadenings $\Gamma_L/2$ and $\Gamma_R/2$. The latter are caused by the coupling of the terminal sites to the adjacent electrodes.

VI. CONCLUSION

In the present article, we clarified a role of metallic electrodes in the transfer properties of a short molecular wire. A model where the current appears as a result of the electron transmission through the LUMOs of two terminal and two interior sites of electron localization within the molecule has been employed. It has been assumed that the LUMO-levels of interior sites are positioned much higher than the electrode Fermi levels, as well as the LUMO-levels of terminal sites. At such a position of the levels, the current through a molecular wire consists of two components associated with the elastic (superexchange) and inelastic (hopping) mechanisms of ET. On the base of the general analytic expression for the current, Eqs. (5)–(10), a detailed analysis of the current behavior has been performed for two limiting cases of strong and weak molecule–electrode couplings. If the noted couplings are strong (large width parameters Γ_L and Γ_R, fast electron hopping between the terminal groups and the adjacent electrodes), then distant one-step D–A hoppings exhibit themselves as the limiting stage of the common charge transfer process in the reference system. Generally, a distant one-step D–A transfer route includes a complicated mixture of the superexchange pathway (the rates k_{DA} and k_{AD}) and the sequential pathway (via the forward (α_D, α, α_A) and the backward (β_D, β, β_A) intersite transfer rates). This is clearly seen from Eqs. (7) and (10). Note, however, that, at a large energy gap between the electronic levels belonging to the interior and terminal sites, the transfer along the superexchange pathway can be more effective than that along the sequential pathway. It happens for a

short molecular bridge connecting the D and A centers [31]. Just such a situation is assumed to be true for a short molecular wire with two interior bridging sites under consideration. Therefore, the condition of fast electrode–terminal site charge hoppings in comparison with slower intrawire charge hoppings is concentrated in inequality [27]). Figure 2 shows the strong rectification effect caused by the nonidentical couplings of the terminal groups to the electrodes. The rectification ratio increases with the ratio of the width parameters. This growth is especially strong when a molecular energy level belonging to the terminal unit is shifted to the Fermi level of the respective electrode. Figure 3 illustrates a pronounced rise of the RR against the applied voltage depending on the values of the width parameters.

In the case of weak molecule–electrode couplings (cf. inequality (31)), the limiting stage of the charge transmission is connected with hopping processes in the interface. Therefore, in line with Eq. (35), just the width parameters Γ_L and Γ_R, as well as the gaps ΔE_L and ΔE_R, become dominant factors controlling the current formation and, thus, the current asymmetry. In the scanning tunneling microsopy (STM), the noted parameters and the gaps can be controlled by the alteration of the distance between the tip and the sample [33]. In our case, it reduces to a variation of the voltage division factors η_L and η_R. When η_L is fixed but η_R is changed, the rectification effect is reached through the variation of the energy gap ΔE_R even though the width parameter is not alternated (see Fig. 4). Note, however, that the variation of the tip-sample distance changes not only the voltage division factors but the respective width parameters. This circumstance has to be taken into consideration if one analyzes the $I-V$ characteristics of a specific molecular wire or a single molecule.

REFERENCES

[1] Joahim, C. & Ratner, M. A. (2005). *PNAS*, *102*, 8801.
[2] Troisi, A. & Ratner M. A. (2006). *Small*, *2*, 172.
[3] Datta, S. (2004). *Nanotechnology*, *15*, S433.
[4] Nitzan, A. & Ratner, M. A. (2003). *Science*, *300*, 1384.
[5] Moth-Poulsen, K. et al. (2005). *Nano Lett.*, *5*, 783.
[6] Haiss, W. et al. (2003). *Am. Chem. Soc.*, *125*, 15294.
[7] Lee, T. et al. (2005). *Curr. Appl. Phys.*, *5*, 213.
[8] Elbing, M. et al. (2005). *PNAS*, *102*, 8815.
[9] Kushmerick, J. G. et al. (2004). *Nanotechnology*, *15*, S489.
[10] Metzger, R. M. (2006). *Chem. Phys.*, *326*, 176.
[11] Chen, J. & Reed, M. A. (2002). *Chem. Phys.*, *281*, 127.
[12] Kondo, M., Tada, T., & Yoshizawa, K. (2005). *Chem. Phys. Lett.*, *412*, 55.
[13] Pati, R. & Karna, S. P. (2004). *Phys. Rev. B*, *69*, 1554191.
[14] Chen, J., Su, J., Wang, W., & Reed, M. A. (2003). *Physica E*, *16*, 17.

[15] Xiao, X., Xu, B., & Tao, N. J. (2004). *Nano Lett.*, *4*, 267.
[16] Grill, L. & Moresco, F. (2006). *J. Phys.: Cond. Matt.*, *18*, S1887.
[17] Yaliraki, S. N., Kemp, M., & Ratner, M. A. (1999). *J. Am. Chem. Soc.*, *121*, 3428.
[18] Karzazi, Y. et al. (2004). *Chem. Phys. Lett.*, *387*, 502.
[19] Stojkovic, S. et al. (2005). *Chem. Phys. Lett.*, *408*, 134.
[20] Kushmerick, J. G. et al. (2002). *Phys. Rev. Lett.*, *89*, 086802.
[21] Tian, W. et al. (1998). *J. Chem. Phys.*, *109*, 2874.
[22] Nitzan, A. (2001). *Ann. Rev. Phys. Chem.*, *52*, 681.
[23] Petrov, E. G. (2005). *Low Temp. Phys.*, *31*, 338.
[24] Petrov, E. G. May, V., & Hänggi, P. (2005). *Chem. Phys.*, *319*, 380.
[25] Petrov, E. G., May, V., & Hänggi, P. (2006). *Phys. Rev. B*, *73*, 0454081.
[26] Petrov, E. G. (2006). *Chem. Phys.*, *326*, 151.
[27] Petrov, E. G. et al. (2006). *Chem. Phys.*, *328*, 173.
[28] Due to polarization effects caused by the metal microelectrodes, the terminal LUMO levels are additionaly shifted to the Fermi levels of the respective electrodes (Unpublished).
[29] Petrov, E. G., May, V., & Hänggi, P. (2004). *Chem. Phys.*, *296*, 251.
[30] Marcus, R. A. & Sutin, N. (1985). *Biochim. Biophys. Acta*, *811*, 265.
[31] Petrov, E. G., Shevchenko, Ye. V., & May, V. (2001). *J. Chem. Phys.*, *115*, 7107.
[32] Zelinskyy, Ya. R. & Petrov, E. G. (2006). *Ukr. J. Phys.*, *51*, 805.
[33] Moresco, F., Meyer, G., & Reider, K. H. (2001). *Phys. Rev. Lett.*, *86*, 127.